

© 2025 IEEE. Personal use of this material is permitted. Permission from IEEE must be obtained for all other uses, in any current or future media, including reprinting/republishing this material for advertising or promotional purposes, creating new collective works, for resale or redistribution to servers or lists, or reuse of any copyrighted component of this work in other works.

CA-Cut: Crop-Aligned Cutout for Data Augmentation to Learn More Robust Under-Canopy Navigation

Robel Mamo¹ and Taeyeong Choi¹

Abstract—State-of-the-art visual under-canopy navigation methods are designed with deep learning-based perception models to distinguish traversable space from crop rows. While these models have demonstrated successful performance, they require large amounts of training data to ensure reliability in real-world field deployment. However, data collection is costly, demanding significant human resources for in-field sampling and annotation. To address this challenge, various data augmentation techniques are commonly employed during model training, such as color jittering, Gaussian blur, and horizontal flip, to diversify training data and enhance model robustness. In this paper, we hypothesize that utilizing only these augmentation techniques may lead to suboptimal performance, particularly in complex under-canopy environments with frequent occlusions, debris, and non-uniform spacing of crops. Instead, we propose a novel augmentation method, so-called Crop-Aligned Cutout (CA-Cut)—which *masks* random regions out in input images that are spatially distributed “around” crop rows on the sides—to encourage trained models to capture high-level contextual features even when fine-grained information is obstructed. Our extensive experiments with a public cornfield dataset demonstrate that masking-based augmentations are effective for *simulating* occlusions and significantly improving robustness in semantic keypoint predictions for visual navigation. In particular, we show that biasing the mask distribution toward crop rows in CA-Cut is critical for enhancing both prediction accuracy and generalizability across diverse environments—achieving up to a 36.9% reduction in prediction error. In addition, we conduct ablation studies to determine the number of masks, the size of each mask, and the spatial distribution of masks to maximize overall performance. The source code is publicly available at <https://github.com/mamorobel/CA-Cut>.

I. INTRODUCTION

Reliable perception capability is essential for Unmanned Ground Vehicles (UGVs) to safely navigate through agricultural fields and perform tasks for precision agriculture. Visual navigation is, however, particularly challenging in under-canopy environments due to factors such as frequent occlusions, debris, and variable spacing of crops (cf. Fig. 2). While deep learning-based methods have been widely adopted to enable perception models to effectively distinguish traversable space from surrounding crops [1], [2], they require large amounts of training data to ensure reliability in real-world field deployment. Unfortunately, data collection is costly, demanding considerable human resources for in-field sampling and annotation.

To address this issue, common image augmentation techniques (e.g., color jittering, Gaussian blur, and horizontal

¹Robel Mamo and Taeyeong Choi are with the Learning and SENSing Research (LaSER) laboratory at Kennesaw State University, Marietta, GA 30060, USA. rmamo@students.kennesaw.edu, tchoi3@kennesaw.edu

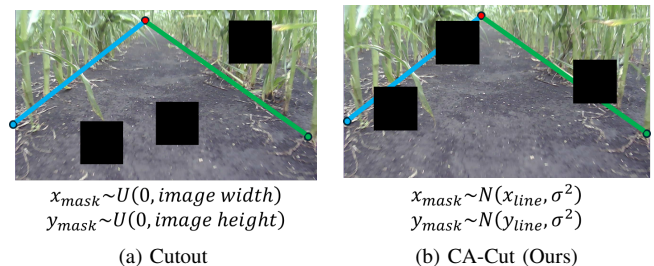


Fig. 1: Conceptual illustration of augmented images by Cutout [3] and CA-Cut in the semantic keypoint prediction task [1], where x_{mask} and y_{mask} represent the randomly sampled central x - and y -coordinates of each mask, and x_{line} and y_{line} denote random x - and y -coordinates sampled on either the blue or green line. Three circles correspond to the vanishing point (red), left (blue), and right (green) intercepts.

flip) are typically applied during model training to ensure robust performance on diversified data [1], [4]. However, in this paper, we hypothesize that relying solely on these techniques may result in suboptimal perception models for under-canopy navigation. Furthermore, we argue that additional manipulations to *simulate* occlusions and structural variability need to be considered in augmenting images. Inspired by Cutout [3], we introduce Crop-Aligned Cutout (CA-Cut), designed to *mask* random regions in input images while distributing them “around” crop rows on the sides (Fig. 1b). In particular, this approach aims to encourage trained models to capture “high-level” contextual features for spatial understanding of crop rows, even in the absence of fine-grained cues of crops. To the best of our knowledge, we are the first to develop masking-based data augmentation techniques for agricultural visual navigation, although it has been often employed in conventional computer vision tasks [5], [6], including agricultural object detection [7], [8].

As shown in Fig. 1, we focus on the *semantic keypoint prediction* problem [1] in under-canopy cornfield environments, detecting three keypoints—the vanishing point of the crop row lines, the intercept of the left crop line with the boundary of the image, and the counterpart of the right crop line. In [1], the authors demonstrated the utility of the predicted keypoints to infer critical information for safe navigation, including the robot’s heading and the distance ratio between crops. To be specific, our experiments with the CropFollow dataset [9] demonstrate that masking-based augmentations (e.g., Cutout [3] and CA-Cut) effectively



Fig. 2: Examples from the CropFollow dataset [9]: (a) severe occlusion, (b) debris and wide spacing in crop rows.

simulate occlusions, enabling perception models to learn robust features for keypoint prediction in visual navigation and outperform ones using only traditional augmentations. In addition, we show that CA-Cut’s masks, *aligned* with crop row lines, play a crucial role in improving both prediction accuracy and generalizability across diverse environments. Moreover, we perform ablation studies to explore different hyperparameters (i.e., the number of masks, the size of each mask, and the spatial distribution of masks) to maximize overall performance.

II. RELATED WORKS

A. Visual Navigation in Agricultural Fields

Visual navigation has been widely explored in the agricultural robotics community to enable autonomous crop monitoring in various crops such as corn [1], [9], sugar beet [4], [10], and vineyards [11]. Recent approaches typically train U-Net-based neural networks [12] on RGB images captured by forward-facing monocular cameras to segment crop rows and generate a traversable reference path for UGVs—either over the canopy [4], [10] or between rows [11], depending on crop height or task requirements. These vision-based systems eliminate the need for additional sensors such as LiDAR, enabling low-cost, energy-efficient deployments.

Instead of segmentation-based methods, the authors in [1] proposed a new type of task—localizing three semantic keypoints (i.e., vanishing, left/right intercept points) in each image—particularly tailored for under-canopy navigation, where color-based pixel-wise segmentation often fails due to occlusions and visual clutter. Their framework, called CropFollow++, used a control module that inferred the robot’s pose based on the predicted semantic keypoints and generated optimal linear/angular velocities to track reference paths. Its effectiveness was demonstrated using physical mobile robots in corn fields with minimal human intervention.

In this paper, we also investigate robot visual navigation in cornfields, leveraging the public dataset from [1], [9]. However, we introduce a novel image *augmentation* method, CA-Cut, aimed at improving the perception module by enhancing robustness in semantic keypoint predictions—ultimately benefiting downstream control modules.

B. Image Augmentation with Masks

Random mask-based image augmentations have shown successful results with improved model generalization in

computer vision tasks. Cutout [3], for instance, was to augment images by applying fixed-size zero masks at random locations in an image and demonstrated consistent improvement across image recognition models. Similarly, CutPaste [6] (CutMix [13]) augments input images by embedding rectangular masks, where instead of zeroing out regions, patches from a random location within the same image (another training image) are pasted into different regions. The authors used this technique to learn structure-sensitive representations for defect detection on industrial items in a self-supervised manner, leveraging a pretext task to classify images with CutPaste from the original. More recently, Colorful Cutout [5] has been introduced, using multi-colored segments within each mask and gradually increasing mask complexity with more colored segments across training epochs to perform curriculum learning.

Inspired by all these, CA-Cut is also designed to erase the content within randomly selected regions to simulate partial occlusion of visual features in training images. However, the key distinction in our work is that the placements of masks are biased toward a certain type of content (i.e., crop rows) which is considered to be visually informative. Moreover, our target application domain is mobile robot navigation, where learning robust perception is particularly critical.

1) *Agricultural Scenarios*: Compared to traditional augmentation methods (e.g., color jittering, flipping, and blur) [1], [14], masking-based augmentation remains underexplored in agricultural vision. For example, the authors in [15] enhanced broccoli head detectors to be robust to occlusion by acquiring training images with intentional partial occlusions by *natural* leaves during data collection. While this approach yielded useful samples, the manual setup limited the scale of augmentation. In [16], cow pose estimation models were developed and evaluated on video frames with zero-value masks that removed parts of cow pixels to test robustness against partial occlusion. Yet, the training itself did not involve such masked images. In [7], Cutout [3] and CutMix [13] were used to augment training image data for wheat head detection, where sampling mask locations were sampled uniformly without any content-aware guidance. A more relevant study to ours is BBoxCut [8], which restricts masks to regions within bounding boxes to occlude parts of wheat heads during detection model training. In contrast, our CA-Cut method is designed for visual navigation in mobile robots and probabilistically places masks both *around* and *directly* on visual cues (i.e., crop rows) by sampling from a biased random distribution. This setup enables random occlusion of *both* precise keypoints and surrounding “contextual” pixels, thereby enhancing robustness to diverse visually challenging scenarios. Similarly, AttMask [17] suggests intentionally masking regions where “teacher” Vision Transformers have attended while training “student” models. By comparison, Our method is more general, imposing no requirements on neural network architecture and offering greater computational efficiency, as it does not necessitate training multiple models such as teacher and student.

III. CA-CUT

A. Random Masking with Spatial Guidance

Both Cutout [3] and CA-Cut augment images by placing zero-valued masks at random locations. Yet, the key distinction is that while the naive version of Cutout [3] is to sample the mask’s location uniformly from $\mathcal{U}(0, \text{image size})$, CA-Cut employs an attraction force that spatially biases the sampling towards the crop rows. As shown in Fig. 1, this design in CA-Cut allows for zeroing out information that is more relevant (e.g., crop parts) to visual navigation rather than random content (e.g., ground, sky, etc.), thereby promoting the learning of more robust models.

CA-Cut is simple and intuitive to implement, leveraging labeled images of crop rows for data augmentation. For example, the CropFollow dataset [9] provides annotated images of cornfields with three keypoints—i.e., the vanishing point, and the intercepts of the left and the right crop rows with the image borders—as visualized in Fig. 1. In this work, we implement CA-Cut using the lines between the vanishing points and these intercepts. For other datasets, alternative labels, such as pixel-wise semantic segmentation [11], may be considered depending on the targeted task.

For each training image, we randomly select either the left or right side to place a zero-valued mask around the corresponding crop row. Then, a random point (x_{rnd}, y_{rnd}) lying on the corresponding line ℓ is sampled and perturbed with an additive white Gaussian noise to center a $(w \times h)$ zero-valued mask around it:

$$\begin{aligned} x_{mask} &= x_{rnd} + \lceil z_x \rceil \text{ and} \\ y_{mask} &= y_{rnd} + \lceil z_y \rceil \\ \text{where } \begin{bmatrix} z_x \\ z_y \end{bmatrix} &\sim \mathcal{N} \left(\begin{bmatrix} 0 \\ 0 \end{bmatrix}, \begin{bmatrix} \sigma^2 & 0 \\ 0 & \sigma^2 \end{bmatrix} \right). \end{aligned} \quad (1)$$

σ is a hyperparameter to control the proximity of generated masks to the lines, measured in pixels. Higher values of σ would lead to masks that are more loosely aligned to the crop rows, whereas lower values keep them more tightly aligned.

For implementation, instead of directly sampling (x_{rnd}, y_{rnd}) on line ℓ , we introduce a random variable $\alpha \sim \mathcal{U}(0, 1)$ and compute:

$$\begin{aligned} x_{mask} &= x_v + \lceil \alpha(x_{inter} - x_v) \rceil + \lceil z_x \rceil \text{ and} \\ y_{mask} &= y_v + \lceil \alpha(y_{inter} - y_v) \rceil + \lceil z_y \rceil, \end{aligned} \quad (2)$$

where (x_v, y_v) represents the vanishing point, and (x_{inter}, y_{inter}) denotes the labeled intercept of the selected line ℓ . Note that x_{mask} and y_{mask} are capped to ensure masks to be located within the image.

B. Multi-mask Augmentation

To learn robust features against severe visual obstructions, we extend augmentation to embed n masks per image, potentially hiding more of the original content to encourage the learning of more robust features. However, placing multiple masks exclusively near crop rows may lead to dense clustering in the same regions, reducing the diversity of augmented images. To mitigate this, we design CA-Cut to

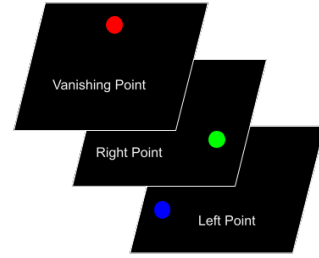


Fig. 3: Ground truth label visualization with three keypoints, each represented in a separate channel. Each channel contains a value of 1 at the keypoint location and 0 elsewhere.

apply k crop-aligned masks and $n - k$ uniformly placed masks, where $1 \leq k \leq n$. Similar to Cutout [3], the uniform placement strategy sets the center of each $w \times h$ mask to:

$$(x_{mask}, y_{mask}) \sim \mathcal{U}(\lceil \frac{w}{2} \rceil, W - \lceil \frac{w}{2} \rceil) \times \mathcal{U}(\lceil \frac{h}{2} \rceil, H - \lceil \frac{h}{2} \rceil), \quad (3)$$

where W and H denote the image width and height, respectively. In Section IV-B, we explore the impact of varying k on overall performance.

IV. EXPERIMENTS

In this section, we first describe specific experimental configurations, including the dataset, model architectures, hyperparameters, and baselines used, to ensure the results are reproducible. Specific results from comparative evaluations will then be presented, accompanied by quantitative and qualitative analyses. Lastly, ablation studies will provide justification for our design choices.

A. Experimental Setup

1) *Keypoint Prediction & Dataset*: We used the CropFollow [9] dataset to train deep-learning models for the three-keypoint prediction task, introduced in [1], throughout following experiments. The dataset contains a total of 25,296 color video frame images captured by mobile robot platforms with RGB cameras while deployed under cornfield canopies in Illinois and Indiana, and each image has a resolution of 1280×720 . However, we have found that only 1,030 images are provided with keypoint labels, so we used only these labeled images for our experiments.

Note that while the authors in [1] evaluated the model performance on the estimated robot’s heading and the distance ratio between the left and right crop rows based on predicted keypoints, our evaluation focuses directly on the keypoint predictions to assess the performance of trained perception model. Specifically, we compute the “Euclidean distance” between each predicted keypoint and its corresponding ground truth location in the original image resolution.

In particular, we also identified *five* distinct sequences within the dataset, presenting various crop growth levels. In addition, some consecutive image frames appear highly similar. Thus, for each sequence, we used the first 80% images for training and the remaining 20% for validation so as

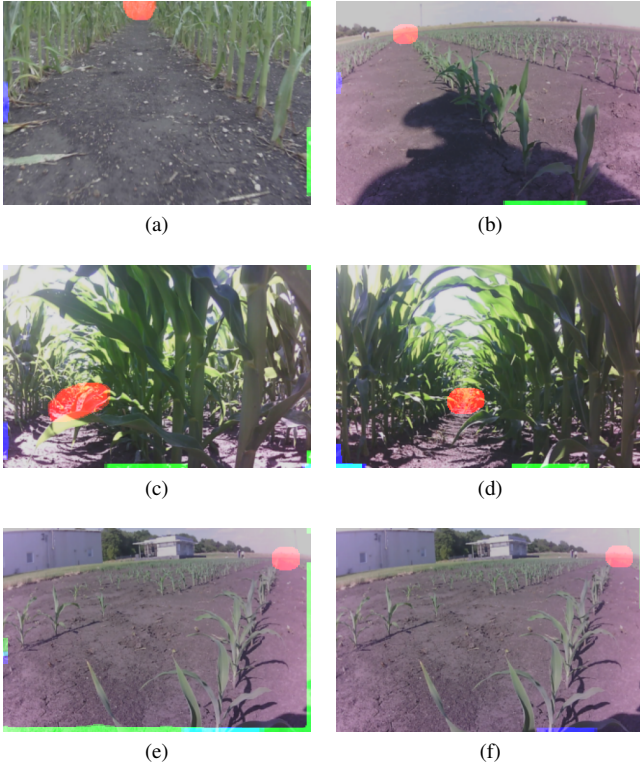


Fig. 4: Examples of keypoint prediction heatmaps—red (vanishing point), green (right intercept), and blue (left intercept)—overlaid on input images for visualization. For visibility, each heatmap was enhanced using OpenCV’s dilation technique [18], applied twice with a (5×5) kernel. (a), (b): CA-Cut’s accurate predictions; (c), (d): CA-Cut’s inaccurate predictions for right keypoints; (e): An outlier case where Cutout yielded large errors (> 600) for both left and right keypoints, while CA-Cut in (f) performed reliably.

to minimize the risk of overestimating the performance and ensure evaluations on “unseen” video frames.

2) *Model Architecture*: To focus only on evaluating the proposed data augmentation technique, we employ an already established model for visual under-canopy navigation with keypoint prediction. To be specific, we used a U-Net-based convolutional encoder-decoder architecture that was adopted in CropFollow++ [1]. The encoder is constructed with a ResNet-18 backbone pretrained on ImageNet [19] to learn to extract informative visual features into a compressed representation. The decoder then utilizes this representation to reconstruct the three keypoints accurately.

Since the code for CropFollow++ [1] is not publicly available, we implemented a similar architecture based on their description. Specifically, the encoder is fed a single input image, resized from 1280×720 to 320×240 and normalized to a $[0, 1]$ range, and consists of four 2D convolutional layers with ReLU activation functions, each followed by a max-pooling layer, with an increasing number of 3×3 kernels: 64, 128, 256, and 512. The decoder has this structure in reverse order, replacing max-pooling layers with upsampling

	CF++	Cutout	CA-Cut			
			$k = 2$	$k = 5$	$k = 8$	$k = 10$
Average	31.4	25.0	22.9	19.8	20.3	22.6
Vanishing	27.7	14.0	17.4	13.3	14.0	14.8
Left	28.8	29.5	24.7	23.0	21.4	24.2
Right	37.7	31.7	26.6	23.1	25.5	28.7

TABLE I: Semantic keypoint prediction errors.

layers to eventually produce a three-channel output image of the same size as the input. Additionally, the 3D feature maps from each encoder are passed to a corresponding layer in the decoder, as designed in conventional U-Nets [20].

The three output channels correspond to the vanishing point, the right intercept, and the left intercepts, respectively. By applying the softmax activation function to each output channel, the model generates spatial likelihood maps for the predicted keypoints. For training, ground truth data is represented as a 3D zero tensor with ones placed only at the corresponding keypoint locations, as illustrated in Fig. 3.

3) *Tested Models & Training Configurations*: To assess the effectiveness of CA-Cut, the following models are trained and validated. Each model is constructed with the identical backbone explained in Section IV-A.2 and applies traditional image augmentation techniques (such as color jittering, Gaussian blur, and horizontal flip) by default:

- **CropFollow++ (CF++)**: Use neither Cutout nor CA-Cut but only traditional image augmentations as in [1].
- **Cutout**: Apply $n = 10$ random masks with no particular spatial distribution guidance [3].
- **CA-Cut**: Apply $n = 10$ random masks, k of which are placed near crop rows using a fixed $\sigma = 100$, while the remaining ones are uniformly sampled.

Masks were sampled after each training image was down-sized to 320×240 . In particular, each mask is of size 60×60 . Note that the specific design choices (e.g., mask size, σ , etc.) are justified in Section IV-D.

In addition, we trained these models with a learning rate of 0.001 and a batch size of 32 for 45 epochs, using the cross-entropy loss function applied to each channel. After each epoch, the model was evaluated on the validation set, and the best-performing model with the minimum loss was saved. We report the average performance over *five* independent training and validation sessions.

B. Comparative Evaluations

Table I shows the average prediction error (i.e., the Euclidean distance between ground truth points and predicted ones), using the original image size. The significantly poorer performance of CF++ *supports* our hypothesis that relying only on traditional image augmentation techniques leads to suboptimal models. In contrast, masking-based augmentations, such as Cutout and CA-Cut, improve prediction quality, implying that artificially generating occlusions is well-suited to under-canopy perception. In particular, the best-performing CA-Cut model ($k = 5$) reduced the error of CF++ by 36.9%.

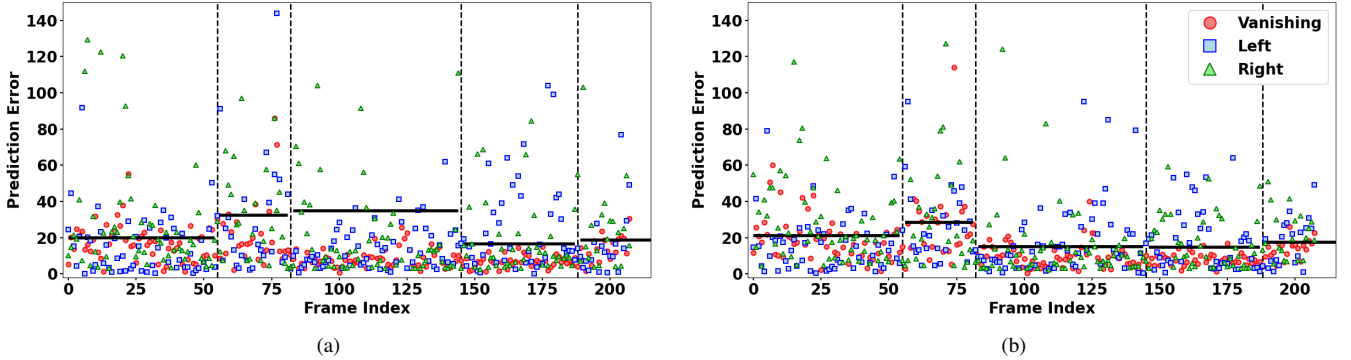


Fig. 5: Video frame-wise prediction errors from (a) Cutout and (b) CA-Cut. Broken vertical lines separate five unique sequences, and each solid horizontal line indicates the average error across all frames within the corresponding sequence. For clarity, six outliers within the range (350, 1,100)—one from sequence 2 and five from sequence 3—are omitted from (a).

Furthermore, compared to using Cutout alone, CA-Cut consistently produced more accurate predictions on average across k values—e.g., for example, achieving a 20.8% average error reduction at $k = 5$. This result suggests that by ensuring to occlude crop row regions during augmentation, CA-Cut enables the model to learn more *robust* features for keypoint localization. Although evaluating the downstream impact on control is beyond the scope of this work, we expect this improvement to translate into even greater gains in “control” performance when keypoint detections are used for robot pose estimation, as in [1], since the 20.8% error reduction applies to each keypoint on average.

Still, masking *only* around crop rows was not optimal, as CA-Cut with $k = 10$ underperformed compared to the more balanced $k = 5$ model. As discussed in Section III-B, this may be because restricting occlusions to crop regions reduces the diversity of the augmented dataset, letting trained models overfit features outside crop row regions.

In addition, Fig. 5 visualizes frame-wise prediction errors for models trained with Cutout and CA-Cut. Compared to Cutout, CA-Cut consistently produced lower prediction errors. Specifically, while Cutout resulted in 22 predictions with errors exceeding 80, CA-Cut had only 11 such cases. This observation further supports our claim that perception models trained with CA-Cut augmentations are more *robust*. In particular, CA-Cut also exhibited lower error variability across sequences compared to Cutout. Cutout produced severe errors ranging from 350 to 1,100 for the second and third sequences, whereas CA-Cut maintained prediction errors below 140 for “all” sequences, highlighting its effectiveness in *generalizing* across diverse environments.

C. Qualitative Analysis

Figure 4a and Fig. 4b show cases where the robot is heading downhill or facing toward the right, which can pose perceptual challenges. Nevertheless, the perception models trained with CA-Cut demonstrated reliable performance, accurately detecting all three keypoints. However, as shown in Fig. 4c and Fig. 4d, CA-Cut can still struggle in leafy

environments from the second sequence, highlighting the need for further investigation to address such conditions.

Figure 4e illustrates an outlier case for Cutout, where prediction errors exceeded 600 for both left and right keypoints. The model was highly confused due to an extreme viewpoint from the far-left corner, where adjacent rows appeared. In contrast, models trained with CA-Cut correctly interpreted the scene and maintained reliable performance (cf. Fig. 4f).

D. Ablation Study

We have first explored various square mask sizes ($w = h$), applying them with Cutout to eliminate any influence of spatially biased mask distribution in CA-Cut. Table II shows that both too small (30) and too large (120) masks degrade performance, and 60×60 is the best choice. The size of 120 might erase too much content to learn useful features. Hereafter, 60×60 will be used for each mask unless mentioned otherwise.

Next, various numbers of masks n per image were tested in Table III, where 10 masks proved most effective on average. Similar to the earlier result, using 20 masks resulted in the worst performance, obstructing too much critical information in the image. Although $n = 5$ also yielded competitive performance, its vanishing point prediction was significantly worse compared to the model using 10 masks.

Lastly, CA-Cut was tested with various σ values (cf. Table IV), when out of $n = 10$ masks, $k = 5$ masks were crop-aligned (cf. Section III-B). $\sigma = 100$ led to the best performance on average. In contrast, removing regions too close to the crop rows ($\sigma = 50$) resulted in the poorest performance, underscoring the importance of occluding *broader* contextual information to enable robust keypoint predictions even when these surrounding cues are obstructed. Moreover, too small σ might lead to densely clustered masks in the same regions, generating similar images and reducing the diversity of augmented images.

Hence, the design choice used in Section IV-B proved to be optimal.

	30	60	120
Average	26.3	25.0	32.0
Vanishing	22.0	14.0	21.9
Left	24.0	29.4	33.0
Right	32.8	31.7	41.1

TABLE II: Prediction errors for Cutout as the mask size varies, using 10 masks.

	5	10	20
Average	26.0	25.0	26.9
Vanishing	20.8	14.0	21.9
Left	25.8	29.4	27.1
Right	31.3	31.7	32.0

TABLE III: Prediction errors for Cutout as the number of (60×60) masks n changes.

	50	100	200
Average	24.2	19.8	21.2
Vanishing	15.5	13.3	19.7
Left	32.5	23.0	19.5
Right	24.6	23.1	24.4

TABLE IV: Prediction errors for CA-Cut with five masks, randomly sampled using different σ values, out of ten (60×60) masks.

to a 36.9% reduction in prediction error. We also discussed

V. LIMITATIONS & FUTURE WORK

While CA-Cut has been designed as a generically applicable data augmentation technique, our experiments were limited to the CropFollow dataset [1], [9]. For future work, we plan to validate our technique on other datasets, including those for sugar beet [10] and vineyard [11], and to explore its applicability to over-canopy and orchard navigation scenarios, as well as to semantic segmentation tasks.

Unlike CropFollow++ [1], where detected keypoints were translated into the robot’s heading and the distance ratio between left and right crop rows, our experiments focused solely on the vision component. This choice was primarily because the robot’s “roll” information captured by the inertial measurement unit (IMU) is unavailable in the dataset, even though it was a key input in their framework. To conduct physical experiments, we will either collect a custom dataset containing all essential information or implement a controller similar to the Segmentation to Proportional Control (SPC) model [11], which does not rely on external IMU data.

VI. CONCLUSION

We have introduced CA-Cut, a spatially guided augmentation technique designed to train robust perception models for visual under-canopy navigation in complex agricultural environments with variable row spacing and occlusions. Through keypoint prediction tasks, we demonstrated the effectiveness of masking-based image augmentations in simulating visual obstructions and improving model robustness. Our results show that biasing the mask distribution toward crop rows in CA-Cut is critical for enhancing both prediction accuracy and generalizability across diverse environments—achieving up

the limitations of this work and future research directions to further enhance model reliability and robustness.

ACKNOWLEDGMENT

This work was partially supported by NSF (2300955) and by USDA-NIFA (2023-38640-39572) through the Southern SARE program (GS24-301).

REFERENCES

- [1] A. Sivakumar, M. Gasparino, M. McGuire, V. Higuti, M. Akcal, and G. Chowdhary, “Demonstrating cropfollow++: Robust under-canopy navigation with keypoints,” *RSS*, 2024.
- [2] T. Wang, B. Chen, Z. Zhang, H. Li, and M. Zhang, “Applications of machine vision in agricultural robot navigation: A review,” *Computers and Electronics in Agriculture*, 2022.
- [3] T. DeVries and G. W. Taylor, “Improved regularization of convolutional neural networks with cutout,” *arXiv*, 2017.
- [4] R. De Silva, G. Cielniak, and J. Gao, “Towards infield navigation: leveraging simulated data for crop row detection,” in *IEEE CASE*, 2022.
- [5] J. Choi and Y. Kim, “Colorful cutout: Enhancing image data augmentation with curriculum learning,” *arXiv*, 2024.
- [6] C.-L. Li, K. Sohn, J. Yoon, and T. Pfister, “Cutpaste: Self-supervised learning for anomaly detection and localization,” in *IEEE CVPR*, 2021.
- [7] Y. Zhang, M. Li, X. Ma, X. Wu, and Y. Wang, “High-precision wheat head detection model based on one-stage network and gan model,” *Frontiers in Plant Science*, 2022.
- [8] K. Seemakurthy, A. A. Opoku, S. D. Bharatula *et al.*, “Bbox-cut: A targeted data augmentation technique for enhancing wheat head detection under occlusions,” *arXiv*, 2025.
- [9] A. N. Sivakumar, S. Modi, M. V. Gasparino, C. Ellis, A. E. B. Velasquez, G. Chowdhary, and S. Gupta, “Learned visual navigation for under-canopy agricultural robots,” *arXiv*, 2021.
- [10] R. De Silva, G. Cielniak, G. Wang, and J. Gao, “Deep learning-based crop row detection for infield navigation of agri-robots,” *Journal of field robotics*, 2024.
- [11] D. Aghi, S. Cerrato, V. Mazzia, and M. Chiaberge, “Deep semantic segmentation at the edge for autonomous navigation in vineyard rows,” in *IEEE IROS*, 2021.
- [12] O. Ronneberger, P. Fischer, and T. Brox, “U-net: Convolutional networks for biomedical image segmentation,” in *MICCAI*, 2015.
- [13] S. Yun, D. Han, S. J. Oh, S. Chun, J. Choe, and Y. Yoo, “Cutmix: Regularization strategy to train strong classifiers with localizable features,” in *ICCV*, 2019.
- [14] T. Choi, O. Would, A. Salazar-Gomez, and G. Cielniak, “Self-supervised representation learning for reliable robotic monitoring of fruit anomalies,” in *IEEE ICRA*, 2022.
- [15] P. M. Blok, E. J. van Henten, F. K. van Evert, and G. Kootstra, “Image-based size estimation of broccoli heads under varying degrees of occlusion,” *Biosystems Engineering*, 2021.
- [16] H. Russello, R. van der Tol, and G. Kootstra, “T-leap: Occlusion-robust pose estimation of walking cows using temporal information,” *Comput. Electron. Agric.*, 2022.
- [17] I. Kakogeorgiou, S. Gidaris, B. Psomas, Y. Avrithis, A. Bursuc, K. Karantzas, and N. Komodakis, “What to hide from your students: Attention-guided masked image modeling,” in *ECCV*, 2022.
- [18] “Eroding and dilating,” https://docs.opencv.org/3.4/db/df6/tutorial_erosion_dilatation.html.
- [19] K. He, X. Zhang, S. Ren, and J. Sun, “Deep residual learning for image recognition,” in *IEEE CVPR*, 2016.
- [20] J. Feng, J. Deng, Z. Li, Z. Sun, H. Dou, and K. Jia, “End-to-end res-unet based reconstruction algorithm for photoacoustic imaging,” *Biomedical optics express*, 2020.